Compressed Sensing (CS) in phase imaging requires dedicated reconstruction strategies

Ukash Nakarmi[1], Shruti Prasad[2], Leslie Ying[1,3], Paul Polak[2], Robert Zivadinov[2,4], and Ferdinand Schweser[2,4]

[1]Dept. of Electrical Engineering, State University of New York at Buffalo, Buffalo, NY, United States, [2]Buffalo Neuroimaging Analysis Center, Dept of Neurology, School of Medicine and Biomedical Sciences, State University of New York at Buffalo, NY, United States, [3]Dept. of Biomedical Engineering, State University of New York at Buffalo, NY, United States, [4]MRI Molecular and Translational Imaging Center, Buffalo CTRC, State University of New York at Buffalo, Buffalo, NY, United States

INTRODUCTION: Quantitative Susceptibility Mapping (QSM) is an emerging new Magnetic Resonance Imaging (MRI) tool for quantitative investigation of tissue magnetic susceptibility [1, 2]. Being the successor of Susceptibility Weighted Imaging (SWI), QSM has many promising applications [3, 4]. However, the requirement of relatively long echo and repetition times (TE/TR) to achieve sufficient contrast-to-noise ratio in the phase part of the complex-valued gradient echo (GRE) signal has hindered this method from finding its way into routine clinical application and large scale research studies. Furthermore, analysis of the intricate echo-time dependence of the phase in white matter, which carries important information about microstructure [5], is critically hampered by the long acquisition times.

Compressed Sensing (CS) [6] achieves signal reconstruction from sub–Nyquist sampled data by exploiting *a priori* information on sparsity in a transform domain. CS has been proven to be a powerful tool in accelerating the data acquisition process in MRI [7, 8]. However, apart from some special applications [13,14], CS in MRI has so far been limited to MRI sequences with negligible phase component [8]. GRE data, used for QSM, has a strong phase component, which carries important information about the magnetic field in the object (Figure 1 top-right). In this case, the reconstruction has to account also for the phase component of the signal (real and imaginary components, Figure 1 bottom), which is not sparse under conventional sparsifying transforms. In this work, we investigate the application of CS for the reconstruction of under-sampled GRE data with long echo times and their characteristics in transform domains. We explore the frontiers and limitations of CS in phase imaging and QSM.

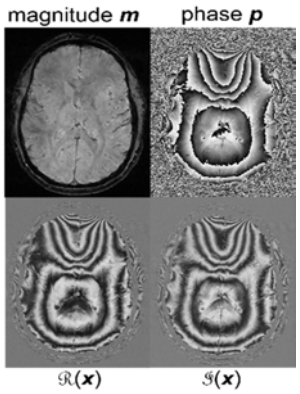

Figure 1. Strong phase component results in substantial variation in real and imaginary images (bottom row).

METHODS: *Data acquisition:* Fully sampled MRI data were acquired on a 3 Tesla GE Signa Excite HD 12.0 (General Electric, Milwaukee, WI) with a multi-channel head and neck coil and a 3D fully flow-compensated GRE sequence with the following sequence parameters: 512x256x64 matrix, 256x192x128mm^3 FOV, 0.5x0.75x2mm^3 voxel size, 75% phase FOV, 12° flip angle, TE/TR 22ms/40ms. Data acquisition time was 8.46 minutes. The raw MRI data (instead of the reconstructed DICOM images) were recorded and used for all further processing steps. *Compressed Sensing*: To mimic sub-Nyquist data acquisition, the fully-sampled data was retrospectively under-sampled using a 2D Poisson disc [9] under-sampling pattern with a reduction factor of 3, resulting in a virtual effective acquisition time of 2.7 minutes. CS image reconstruction [7] was obtained by solving the following (conventional) constrained optimization problem (Method 1):

$$\boldsymbol{minimize}: \boldsymbol{\lambda_1}\|\boldsymbol{\Psi I}\|_{l1} + \boldsymbol{\lambda_2 TV(I)}, \boldsymbol{s.t.}\|\boldsymbol{Y} - \boldsymbol{F_{u3}I}\|_2 < \boldsymbol{\epsilon}\ ^{(1)},$$

where, $\boldsymbol{Y}$ is the undersampled 3D k-space data, $\boldsymbol{F_{u3}}$ is a partial 3D Fourier transform operator and $\boldsymbol{I}$ is the reconstructed 3D image. $\boldsymbol{\Psi}$ and $\boldsymbol{TV}$ are the 3D wavelet operator and the total variation operator, respectively. Both operators work separately on the real and imaginary signal parts. Minimizing l_1 norm and TV norm promotes sparsity on real and imaginary parts of the complex-valued images. $\boldsymbol{\lambda_1}$ and $\boldsymbol{\lambda_2}$ are regularization parameters. In addition, a special CS reconstruction method that includes a phase smoothing prior was implemented (Method 2) [13,14]. *Effect of phase on CS reconstruction*: We carried out dedicated experiments to investigate the impact of a strong phase component on the CS reconstruction with methods 1 and 2: We mimicked MRI data with negligible phase by creating a second model from the same acquisition and manually set the phase component to zero. We then compared the CS reconstruction of this dataset with the reconstruction of the dataset that contained the strong phase components (Figure 2). *Analysis*: Reconstructed phase images from Method 1 were unwrapped using a best-path unwrapping algorithm [10] and background field corrected using SHARP [11] (radii 0.5 to 5mm). Susceptibility maps were calculated from the background corrected phase images using the HEIDI algorithm [12].

RESULTS: Figure 2 compares CS reconstruction of the two models. While the reconstruction quality is high in the magnitude-only model, the reconstruction of the complex model lacks definition of tissue interfaces (e.g. white and gray matter) and shows considerable inhomogeneities. However, we can see that these methods are still not suitable when phase itself is not smooth and contains many structures and fine details. Figure 3 compares phase (left-most and middle column) and QSM (right-most column) reconstructed from fully sampled (top row) and undersampled data (middle row, Method 1), respectively. The images resulting from the CS reconstruction suffer from granular inhomogeneity similar to those seen in Figure 2. In both the phase and the QSM, the white-gray matter interfaces and small venous vessels are almost indiscernible on the CS reconstruction, which is also reflected by structural information in the difference patterns.

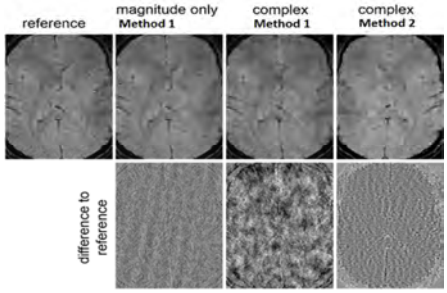

Figure 2. Effect of phase on magnitude images resulting from CS reconstruction. From left to right: Reference, CS reconstruction of magnitude-only model using Method 1. CS reconstruction with Method 1 and Method 2 of GRE data with strong phase. *CS reconstruction of GRE data with strong phase results in poor magnitude reconstruction.*

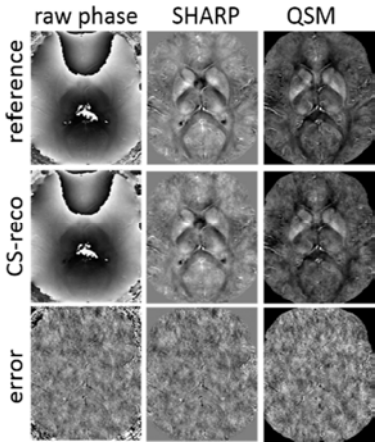

Figure 3. Reconstruction of phase images with Method 1 and impact on subsequent quantitative phase analysis. From left to right: raw wrapped phase, background corrected phase, QSM. *CS reconstruction suffers from significant loss of anatomical detail*.

DISCUSSION: Our work demonstrates that available CS reconstruction strategies are not applicable to GRE acquisition with long echo times, as required for QSM. Poor CS reconstruction obtained from the complex-valued data can be attributed to the sparsity enforcing terms (see $\boldsymbol{\Psi}$ and $\boldsymbol{TV}$ above), which neglect the structural information contained in the phase component of the complex-valued images. These terms enforce sparsity in the real and imaginary parts of the signal, although real, imaginary signals are not necessarily sparse under TV, and wavelet transforms in these data (see Figure 1). Some algorithms have recently been presented that enforce sparsity of magnitude and phase separately in complex-valued signals [13, 14]. However, these approaches rely on the fundamental assumption that the phase is (locally) smooth (such as Method 2). This assumption is not a valid assumption for GRE data with long echo times (see Figure 1).

CONLUSION: A critical need exists to extend CS toward data with substantial structural information in the phase component. Dedicated reconstruction strategies are required that account for, and preserve the important phase information in GRE MRI with long echo times.

REFERENCES: [1] Young, I.R., et al., *J Comput Assist Tomogr*. 1987. [2]. Holt, R.W., et al. J MRM 1994. [3]. Schweser, F., et al., *Neuroimage*, 2011 [4]. Chen, W., et al., 2013. [5] Sukstanskii,A.L,et.al,*MRM*,2014. [6]. Donoho, D.L., *IEEE Transactions*, 2006(4) p.1289 [7]. Lustig, et al., *MRM*, 2007 [8]. Liang, D., et al.,*MRM*, 2009 [9] Bridson, R., *ACM SIGGRAPH 2007*. [10]. Abdul-Rahman, H., et al., *Appl Opt*, 2009 [11] Topfer, R., et al., *MRM*, 2014. [12]. Schweser, F., et al, *NeuroImage*, 2012 [13]. Zhao,F.,et al., *IEEE Trans Med Imaging*, 2012 [14]. Zibetti, M.V.W, et al., *ISBI* 2010